Astron. Astrophys. 319, 260–266 (1997)

ASTRONOMY
AND
ASTROPHYSICS

Detection of circumstellar dust shell around the supergiant TV Geminorum from milliarcsecond resolution near-infrared observations

Sam Ragland, T. Chandrasekhar, and N.M. Ashok

Physical Research Laboratory, Navrangpura, Ahmedabad-380 009, India (e-mail: sam@prl.ernet.in)

Received 25 October 1995 / Accepted 22 July 1996

Abstract. A lunar occultation of the M1 supergiant TV Gem has been observed in the near infrared region at 2.2 μm. A detailed analysis of the observed occultation light curve has been performed using two different reduction methods permitting the circumstellar dust envelope to be directly detected for the first time around TV Gem. The star has been resolved to yield a uniform disk diameter of 4.9$\pm$0.3 milliarcseconds (mas) and the stellar effective temperature has been derived to be 3670$\pm$125 K. Its circumstellar dust envelope has a radius of $\sim 20\,R_\star$ with star to shell flux ratio of ~ 35 at 2.2 μm. A simple radiative transfer dust shell model constrained by our occultation observations, 9.7 μm silicate emission feature strength and far IR excess seen in IRAS observations shows that the dust is probably restricted to two well separated dust shells – the inner shell is at a radial distance of $\sim 20\,R_\star$ and the outer one is at $\sim 500\,R_\star$. Sporadic dust condensation in TV Gem as in the case of α Ori is suggested.

Key words: stars: TV Gem – circumstellar matter – supergiants – stars: fundamental parameters – infrared: stars

1. Introduction

As stars evolve from the main sequence onto asymptotic giant branch of the Hertzprung-Russell (HR) diagram they exhibit mass loss which can be due to cool winds (Salpeter 1974), thermal pulses (Schwarzschild & Härm 1962) or some other types of mass ejection. It is known that the dust formation is intimately related to mass loss, but little direct evidence exists about the dust forming zone. Observing evolved giants and supergiants in the infrared with sufficiently high angular resolution (HAR) to resolve the stellar surface and immediate surroundings can answer some of the most interesting questions related to grain condensation, mass loss and hence stellar evolution. Lunar occultation is a powerful and productive technique at present for achieving HAR particularly in the near infrared region, because of the reduced background of scattered moon light compared to the optical region. The technique consists of recording the straight edge diffraction pattern of the star light produced by the sharp edge of the moon and obtaining HAR by mathematical modelling. The most attractive aspect of the method is its ability to achieve high one dimensional angular resolution down to 1$-$2 mas with an accuracy which can be as high as ~ 0.1 mas (Ridgway 1977; Richichi et al. 1988). However careful consideration of various factors like optical bandwidth of the filter used, telescope aperture and time constant of recording system that influence the occultation light curve is necessary before such HAR can be achieved in practice.

It has been known for long that cool giants of spectral type M or later have circumstellar gas shells (Deutsch 1960). Gehrz & Woolf (1971) and Gillett et al. (1971) have shown from 10 μm observations that many shells have dust component as well. However direct observations of these shells around red giants have been very limited. Recent observations in the infrared with a spatial interferometer (Danchi et al. 1994; Townes et al. 1994) on the distribution of dust around a sample of well known late type stars have shown that these stars fall into two catagories – one class has inner radii of dust shells very close to the photosphere (3$-$5 stellar radii) and at a higher temperature ($\sim$ 1200 K) than previously measured. This class includes VY CMa, NML Tau, IRC+10216 & o Ceti. To this class also can be added the bright carbon star TX Psc in which an asymmetric distribution of warm dust at a few stellar radii has been reported recently (Richichi et al. 1995). The second class of stars has dust shells with large inner radii ($\geq$ 8 stellar radii) and very little dust close to the star. This class includes several supergiants α Sco, α Ori and α Her. Interestingly SiO, H_2O or OH maser emission is not seen in these supergiants while it is generally present in the other class. There is also good evidence that for long period variables like o Ceti new dust is formed in the cooling phase close to the star, during each cycle. Recent theoretical work by Winters et al. (1995) on the circumstellar dust shell around long period variables predicts discrete shell-like distribution of dust across the circumstellar shell around carbon stars. For super-

Send offprint requests to: S. Ragland

Table 1. Predicted circumstances of observed event

Date	30 March 93
Time (UT)	14:30:28
Predicted position angle (deg)	95
Predicted contact angle (deg)	11
Lunar phase (days since new moon)	7.1
Altitude (deg)	59.4
Shadow vel. comp. ($km\,s^{-1}$)	0.6456

Table 2. JHK photometry of TV Gem

Filter band	J	H	K
Magnitude	2.13 ± 0.05	1.17 ± 0.1	0.93 ± 0.05

giants like α Ori which is a irregular variable gas and dust are emitted episodically and there may not be any dust production for many decades. In this context it is worth while to study other supergiants at HAR to investigate the nature of the dust shells.

A program of observing lunar occultations in the near infrared ($1-5\,\mu$m) is in progress at the Physical Research Laboratory, Ahmedabad, India to investigate the circumstellar dust envelope around late giants and supergiants. Several occultations have been successfully observed mainly in the K band. A rare opportunity to observe the lunar occultation of M1 supergiant TV Gem was successfully utilized. In this paper we report the detection of a circumstellar dust shell around the star consistent with the strong silicate emission feature and far infrared excess seen in IRAS observations.

2. Observations

The lunar occultation observations presented here were carried out at the 0.75 m telescope at Kavalur (78°, 49′ 45″E, 12° 34′ 35″N, 725 m) during early 1993. Table 1 lists the circumstances of the event. Event prediction was computed with a code developed by us which is accurate to few seconds. The occultation event reported here was a disappearance event at the dark limb of the moon.

The instrument used was a LN_2 cooled InSb based high speed infrared photometer, the design of which is described in Ashok et al. (1994). Occultation light curve presented here was observed in the standard K filter ($\lambda = 2.2\,\mu$m, $\Delta\lambda = 0.4\,\mu$m). A 2 mm circular diaphragm was used which corresponds to 42″ field on the sky. Data sampling was at a rate of 1 kHz for 30 seconds using a 16 bit high speed A/D converter (Keithley system 575). The absolute timing of the event was not recorded, since it is not relevant for the present work.

Near infrared photometry of TV Gem has been carried out using the same high speed IR photometer with 1.2 m telescope at Gurushikhar (72°47′E, 24°39′N,1680 m) and is listed in Table 2.

3. Data analysis

Data analysis was performed using two different methods. The first method is the standard nonlinear least squares (NLS) technique introduced by Nather & McCants (1970) and the second method is a model independent algorithm (MIA) introduced by Richichi (1989) for occultation work. In the case of NLS, a model is assumed for the one dimensional brightness distribution of the source (along the direction of occultation) with a set of physical parameters and the problem is to obtain best statistical estimations for these parameters along with other scaling parameters like source intensity, background intensity, velocity component of the moon along the direction of occultation and the time of geometric occultation. Uniformly illuminated stellar disk model is assumed for TV Gem which has the functional form,

$$S(\phi) = I_o \frac{2}{\pi} \left[1 - \left(\frac{\phi}{\Omega} \right)^2 \right]^{\frac{1}{2}} \tag{1}$$

where Ω is the stellar angular radius and I_o is the stellar intensity.

The data reduction using NLS method can be used to model complicated geometry for the stellar photosphere and the circumstellar dust envelope. However, the NLS method demands the knowledge of the geometry of the source which is not always possible in practice. In such cases, MIA can be advantageously used. MIA is a composite algorithm which makes use of the NLS method and Lucy's deconvolution algorithm wherein a guess profile is assumed for the brightness profile of the source and is iteratively modified to obtain a better fit for the data.

Averaging effects due to finite optical filter bandwidth and telescope aperture have also been accurately taken into account. The analysis takes into account the CVF spectrum of TV Gem reported by Arnaud et al. (1989) in the spectral range 2–2.4 μm while accounting for the smearing effect caused by the finite optical filter bandwidth.

The frequency response of the detector system used is not flat upto the sampling cutoff frequency of occultation observations. Hence system time response to a transient light pulse is experimentally determined accurately and is used in our data reduction procedure to account for this instrumental averaging effect.

4. Results and interpretation

4.1. Direct detection of dust shell

Observed occultation light curve of TV Gem, fitted with a simple uniformly illuminated disk stellar model does not yield a satisfactory fit. The nature of the residuals suggests that the model fit is likely to improve if an extended source is present in addition to the central star. Since the nature of the extended source is not known, MIA has been used to obtain the shell brightness profile. We decompose the model light curve into stellar and shell components. For the stellar component a uniformly illuminated disk model is assumed, while for the shell a flat guess profile is assumed. The shape and the extent of this

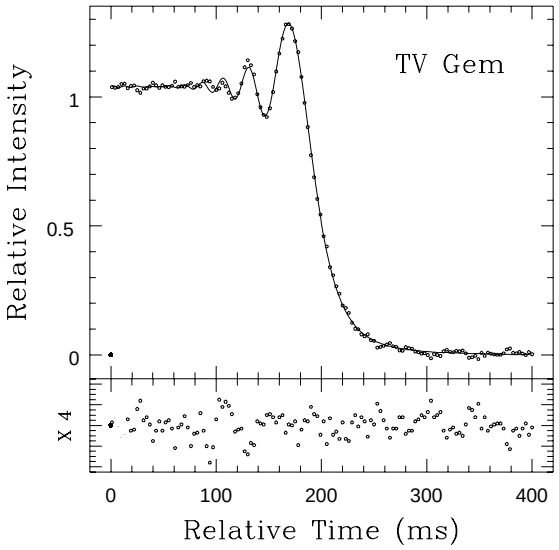

Fig. 1. Occultation light curve of TV Gem (dots) fitted using MIA (solid line) is shown in the upper panel. Lower panel shows the residuals of the fit enlarged by a factor of 4

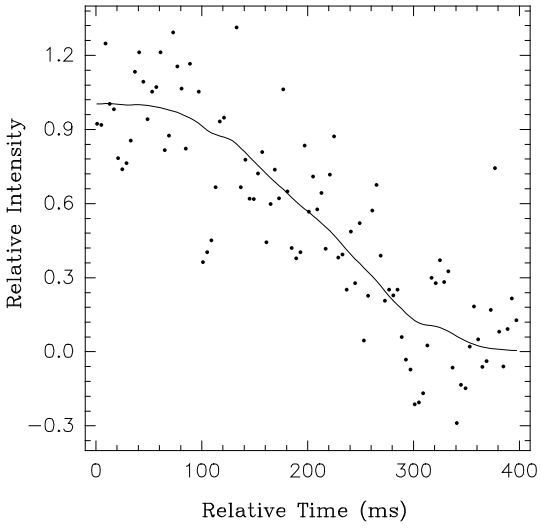

Fig. 2. The contribution to the light curve of TV Gem due to the extended component alone recovered using MIA (dots) and the corresponding fit (solid line)

guess profile assumed for the shell is not critical to achieve convergence, except that, the extent should be larger than the true extent of the circumstellar envelope present in the data. First, NLS fit is carried out to estimate the stellar angular size and the star to shell flux at 2.2 μm along with the scaling parameters. Now, the stellar component is removed from the observed light curve and Lucy's deconvolution algorithm is used to modify the shell brightness profile. A three point binning of the data is made to improve the signal to noise ratio while performing Lucy's deconvolution which sets the angular resolution of the recovered brightness profile at $\sim$ 1.1 mas. The whole procedure is repeated till it converges. Five iterations of the MIA algorithm are sufficient to achieve good fit to the data.

The data fitted using MIA is shown in Fig. 1. The shell component of the observed light curve and the corresponding model fit are shown in Fig. 2.

The recovered brightness profile for the source is shown in Fig. 3. The broad feature recovered is well above the noise level and is the signature of the dust shell around the central star. The shape and the amplitude of this recovered profile is very stable against initial guess values of the model fitting procedure.

Figure 4 shows the residuals (data $-$ model) for (a) a uniform disk model using NLS and (b) a uniform disk plus circumstellar shell model using MIA. It can be seen that the uniform disk model has an oscillatory residue pattern which is indicative of an unaccounted more extended source. The residuals after invoking circumstellar extended feature do not exhibit this oscillatory pattern and the noise pattern is now random. The solid lines drawn in Fig. 4 are not due to any least squares fitting and are plotted to merely show that inclusion of a shell makes the residue more random.

The recovered brightness profile is fairly symmetric. For the best fit model we derive the FWHM of the shell extent to be 100 $\pm$ 20 mas and the star to shell flux ratio at 2.2 μm to be 35. The

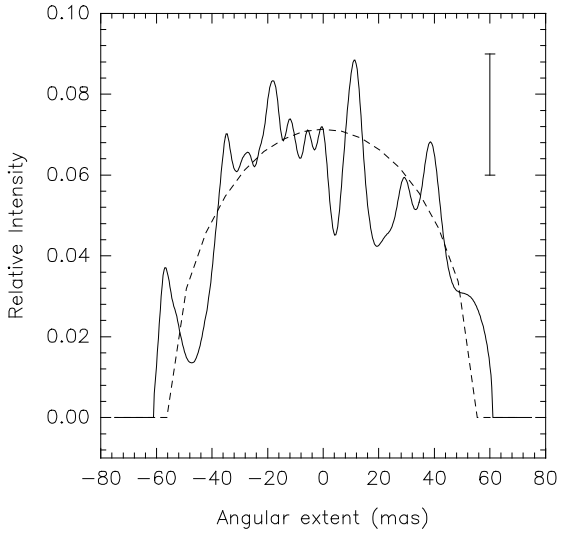

Fig. 3. The recovered brightness profile of the extended component of TV Gem (solid line) recovered using MIA. Also shown is a uniform disk brightness profile of 55 mas angular radius (dashed line). Also shown is an errorbar taking into account the noise level in the data

derived value for the stellar angular diameter is 4.9$\pm$0.3 mas. U, B & V photometric values of TV Gem are corrected for the presence of a companion (Underhill 1984). Bolometric flux has been derived by integrating numerically the available optical and infrared photometric data in the literature (Hoffleit & Jaschek 1982; Underhill 1984; Gezari et al. 1993) in addition to our JHK values. Thus derived value for the bolometric flux for TV Gem is 1.53×10^{-6} erg cm^{-2} s^{-1} and the estimated error in this bolometric flux is 10%. From the derived stellar angular size and bolometric flux, we derive an stellar effective temperature of 3670$\pm$125 K for TV Gem.

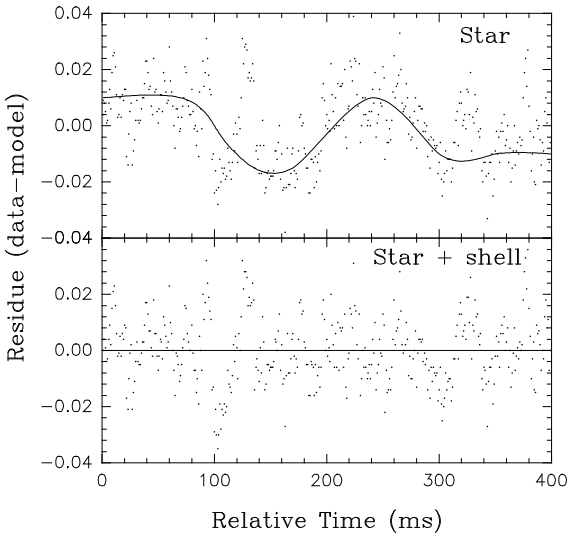

Fig. 4. Residuals of the 'star only model' using NLS is shown in the upper panel and the lower panel shows the residuals of the 'star plus shell model' using MIA

4.2. An observational history of TV Gem and its surroundings

TV gem is a distant oxygen rich supergiant classified as M1 Iab. It is a short period semi regular pulsating variable of variability type SRc with a period of 182 days (Kukarkin 1969). The best estimation of distance to TV Gem is based on interstellar extinction towards eleven stars in the Gem OB1 association to which the star belongs. This yields a value of 1200 pc with an uncertainty of $\sim$ 25 % (Underhill 1984). The estimated value for the visual extinction is 1.98 magnitude (Radick et al. 1984). The visual magnitude given by Hoffleit & Jaschek (1982) and most widely used is 6.56. However, Keenan (1989) gave a value 7.0–7.8 for the visual magnitude and the spectral classification M0−1 Iab.

TV Gem is a suspected syncretic binary (Buss & Snow 1988) where the primary is the early M supergiant and the secondary is a early B star. Syncretic (VV Cep) type binaries are a loosely defined class of spectroscopic binaries which exhibit a composite spectrum of an early M supergiant and a hot companion. The hot star orbits inside the stellar wind region of the primary.

The IUE low resolution spectrum in the range 1000–3000 Å shows a clear bump at 2175 Å and Si II, Si III, C II, Si IV, Al II absorptions (Buss & Snow 1988). Based on IUE data and UBV photometry, Underhill (1984) has suggested a B 3.5 IV companion around the M1 Iab supergiant primary. They estimate an angular separation between the two stars to be $\sim$ 3 arcseconds with a B magnitude difference of 1.6. So far the presence of the companion has not been observationally established by direct imaging. We estimate the magnitude difference in K magnitude between these components to be $\sim$ 6. The secondary, even if present, will be lost in the noise and hence we can't confirm or deny its presence from our occultation observations.

TV Gem has earlier optical occultation observations using y strömgren filter (Radick et al. 1984). The derived value for the stellar angular diameter is 5.31 $\pm$ 0.91 mas. Our value for the stellar angular diameter of 4.9 $\pm$ 0.3 mas is well within the quoted errors of the previous measurement and is also more accurate due to better S/N on the account of lesser background scattered light level in the K band. Recently, it has come to our notice an unpublished occultation light curve of TV Gem in the K band observed by Richichi (1995). The derived value for the stellar angular diameter from this light curve is consistent with our value.

The circumstellar gaseous environment of TV Gem has been studied in the CO (1−0) and CO (2−1) lines in the millimeter region (Loup et al. 1993; Heske 1990). The velocity profile in the CO (1−0) line is weak and flat topped which appears unresolved in the beam width of observations of $\sim$ 23 arcsecond. This is not surprising as the CO envelope size (R_{CO}) limited by the ambient interstellar radiation field is typically 10^{17} cm $< R_{CO} < 6\times10^{17}$ cm for optically thin cases (Loup et al. 1993). At the distance of 1200 pc assigned to TV Gem for the derived value of $R_{CO} = 1.7 \times 10^{17}$ cm one obtains for the envelope an angular size of 9.7 arcseconds which is well below the beam width of the observations. From the CO velocity profile, an expansion velocity (V_e) of 12 km s^{-1} has been derived. The mass loss rate ($\dot{M} \propto V_e^2\ d^2$) for a distance of 1200 pc to the source is 2×10^{-6} $M_\odot$ yr^{-1}, assuming a [CO/H_2] ratio of 5×10^{-4} typical of oxygen rich stars.

Stencel et al. (1989) have studied the infrared fluxes, spatial and spectral characteristics of over a hundred supergiants including TV Gem. They find that about one fourth of these objects are spatially resolved in the coadded (ADDSCAN) IRAS data at 60 μm and possess extended circumstellar shells with implied expansion for $\sim 10^5$ yr at a typical rate of $\sim$ 10 km s^{-1}. Empirically the IRAS point source response function at 60 μm is 2.3–2.5 arcminutes in terms of full width at 10% of the maximum intensity ($W_{10\%}$). With this criterion, TV Gem is just resolved at 60 μm with a full width at 10% value of 2.9 arcminutes. It must be pointed out, however, that Young et al. (1993) have examined IRAS 60 μm and 100 μm data for spatially resolved structure in a large number of stars. TV Gem does not figure in their final list of resolved objects as in their classification, it falls into a set of stars which are near other sources or embedded in regions of extended emission resulting in curved base lines. Hence, there is no conclusive but conflicting evidence of the extended source structure around TV Gem from IRAS imagery at the level of arcminutes. However, the 9.7 μm silicate emission feature seen in IRAS LRS and the infrared excess present in the IRAS photometric data for TV Gem unambiguously point to the presence of a dusty circumstellar shell.

It is known from early broad band IR observations that onset of silicate excess in oxygen rich stars is seen for all stars later than M6 III, M5 II, M1 Iab, K3 Ia and Go Ia−0 (Merrill & Stein 1976). Supergiants redder than V−K $\sim$ 6 invariably exhibit silicate feature. Many warmer supergiants with V−K $<$ 6 have IR excess as shown by the ratio ($\frac{f_{25}}{f_{12}}$) indicative of dusty circumstellar envelopes but do not generally exhibit a silicate feature. However, as shown by Stencel et al. (1989) the broad band warm dust indicator ($\frac{f_{25}}{f_{12}}$) peaks among these stars with

lowest LRS continuum ratio. Cooler stars have more dust. The cooler photosphere and the greater quantity of dust contribute to a shallower LRS continuum. The emission strength of the feature at 9.7 μm is also known to correlate with ($\frac{f_{25}}{f_{12}}$) ratio because both relate to newly formed warm dust. TV Gem is an exception to the rule or a border line case where both IR excess and silicate feature are present although the V−K value is 5.6. We estimate the mass loss rate from the 9.7 μm silicate feature strength (Skinner et al. 1988) to be $\dot{M} = 1.8\times10^{-6} M_\odot\ yr^{-1}$, which is consistent with that derived from CO observations.

4.3. Circumstellar dust distribution

The dust distribution around TV Gem is investigated taking into account our occultation observations, 9.7 μm silicate feature seen in the IRAS LRS and the 12, 25 and 60 μm far infrared fluxes from IRAS. A simple radiative transfer model of an optically thin isothermal shell composed of grains of a single size is invoked.

The following are the observational constraints imposed in the model:

1. The radius of the dust shell around TV Gem derived from our lunar occultation data analysis is 20±5 $R_\star$.
2. The estimated value for the shell flux at 2.2 μm is 5.7×10^{-16} W cm^{-2} μm^{-1}.
3. In addition, the shell flux at 9.7 μm, 12 μm, 25 μm and 60 μm are estimated from IRAS data by subtracting stellar contribution which is calculated from the stellar parameters derived from our occultation light curve. These fluxes are respectively 3.6×10^{-16}, 1.7×10^{-16}, 1.7×10^{-17} and 4.1×10^{-19} W cm^{-2} μm^{-1}. The stellar contribution to the total flux at these wavelengths are in the range 15–22 %.

The flux (F_λ) at wavelength λ is given by

$$F_\lambda = \frac{4\pi a^2 Q_{\rm emit} B(\lambda, T)}{4\pi d^2} N, \qquad (2)$$

where B(λ,T) is the Planck function (blackbody flux) at temperature T and wavelength λ, d is the distance to the source, N is the total number of grains in the shell and Q_{emit} is the emission efficiency of the grain. We assume the grains to be bare silicates without mantles. The spectral signature of the silicate features at 10 and 20 μm are characteristic of the Si-O stretch and bend in rocky materials. Recently, there has been considerable discussion on the definition of true astronomical silicate in an interstellar sense. Greenberg & Li (1995) have interpreted 9.7 μm and 18 μm interstellar features not in terms of pure silicate but by a pure silicate core-organic refractory mantle grains. While this core-mantle model provides a better fit to the interstellar absorption 10 μm feature, for regions of grain formation relatively close to the stellar photosphere, wherein 10 μm silicate feature is in emission, a bare silicate model may be adequate. Accordingly, Drain & Lee (1984) model to obtain Q_{emit} values in the region of interest has been used. A constant grain size of a = 0.1 μm and a grain density of 3.3 gm/cc (Skinner 1987) are assumed.

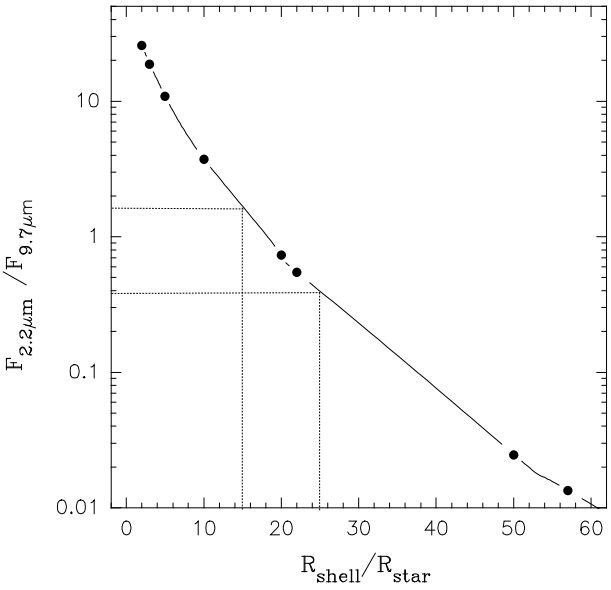

Fig. 5. Calculated 2.2 μm to 9.7 μm flux ratio as a function of radial distance from the central star using a simple radiative tranfer shell model

Assuming radiative equlibrium in the circumstellar environment, the shell flux ratio (2.2 μm to 9.7 μm) as a function of radial distance from the star is computed using eqn. 2 and shown in Fig. 5. It can be seen that the flux ratio in the range 0.4−1.8 corresponds to a shell radius in the range 15–25 $R_\star$. Even taking into account the errors involved in the estimation of shell flux value at 2.2 μm from our occultation observations, the actual ratio is expected to lie well within this range. The conclusion is that the dust shell radius is sharply confined to the zone 15–25 $R_\star$. These results also suggest that both 2.2 μm and 9.7 μm fluxes mainly arise from the same dust zone existing at $\sim 20 \pm 5\, R_\star$.

The shell maximum temperature can range from $\sim$ 950 K at 15 $R_\star$ to $\sim$ 730 K at 25$_\star$. There exist no agreement on the precise condensation temperature of silicate dust grains (Griffin 1993). Some authors favour values as high as 1500 K (Volk & Kwok 1988), others a value of 1000 K (Skinner & Whitmore 1988; Danchi et al. 1994), while a value as low as 500 K was used as the inner dust shell temperature of some stars (Rowan-Robinson & Harris 1983; Hagen 1982; Onaka et al. 1989). Refractory compounds condense first in the ejected hot gas envelope, close to the central star as their condensation temperature is high. The compounds of Al, Ti, Ca and probably Fe will form the seed of the grains. The condensation temperatures of Al_2O_3, $CaTiO_3$, $Ca_2MgSi_2O_7$ & Metallic Fe are respectively 1720 K, 1650 K, 1580 K & 1450 K. These 'seed' nuclei subsequently grow by becoming clad by more abundent Mg-silicates which condenses at relatively lower temperature. The condensation temperature of Mg_2SiO_4, Mg_2SiO_3 & SiO_2 is 1350 K (Turner 1991).

We now consider a uniform dust mass loss rate of $2\times10^{-8} M_\odot$ and an expansion velocity of 10 km s^{-1} for the circumstellar material around TV Gem, consistent with CO obser-

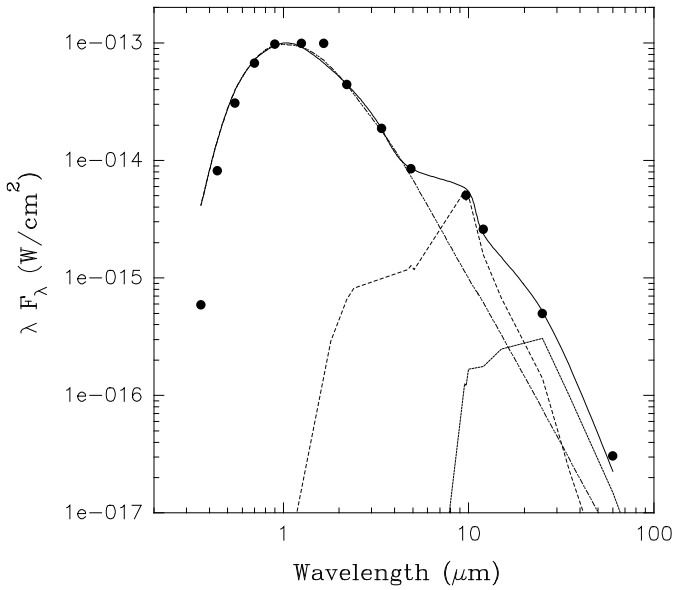

Fig. 6. Observed photometric values (dots) fitted with a three component (star + double shell) model is shown. In addition to our measured near infrared photometric values (this paper), values are also taken from the literature (Hoffleit & Jaschek 1982; Underhill 1984; Gezari et al. 1993). The spectra of the individual components are shown as dashed lines

vations in the outer regions of TV Gem (Loup et al. 1993; Heske 1990). The number density of silicate grains, for this situation has a R^{-2} dependence and can be written as

$$n\,(R) = \frac{3.18 \times 10^{-3}}{\left(\frac{R}{R_\star}\right)^2}\ \mathrm{cm}^{-3}. \qquad (3)$$

The model flux from the shell with boundaries R_1 and R_2 are estimated by integrating between the limits R_1 and R_2 using eqn. 2 & 3. Although the observed shell flux at 2.2 μm and 9.7 μm can be explained with the inner dust shell detected from our occultation light curve, the far infrared excess, particularly at 60 μm, can be fitted only by invoking cooler dust at $\sim 500\,R_\star$. There is no evidence of dust in the intermediate region (Fig. 6). An immediate conclusion of this confinement of dust to two isolated shells is that the dust condensation in TV Gem and the consequent mass loss is not a continuous process. While the void in the inner zone $\leq 15\,R_\star$ can be attributed to temperatures higher than the condensation temperature of silicate material, the absence of material beyond $25\,R_\star$ can only be explained by considering the mass loss rate in TV Gem to be a sporadic process. The dust seen in the 15–25 $R_\star$ zone has an estimated mass of $\sim 10^{-7}$ $M_\odot$ from its 2.2 μm shell flux values and it would have formed in a time frame of a few decades. The mass estimated for the cooler outer shell is 6×10^{-6} $M_\odot$ with a shell thickness of $\sim 200\,R_\star$. It would have condensed $\sim 10^3$ yrs back.

Finally we compare our results on the circumstellar dust shell around TV Gem with that of α Ori, since both the supergiants are of similar spectral and luminosity class. The dust shell around α Ori has been studied in great detail with various interferometric observations (Sutton et al. 1977; Howell et al. 1981; Roddier & Roddier 1983; Bloemhof et al. 1984; Bloemhof et al. 1985; Christou et al. 1988; Danchi et al. 1990; Bester et al. 1991). Recently, Danchi et al. (1994) reported two dust shells present around α Ori – one at $\sim 25\,R_\star$ with a shell thickness of $\sim 2\,R_\star$ and inner shell temperature of 381 K and the other at $\sim 50\,R_\star$ with a shell thickness of $\sim 5\,R_\star$ and inner shell temperature of 266 K from infrared spatial interferometric observations suggesting a sporadic dust condensation in α Ori. We suggest that the circumstellar dust shell properties of these two supergiants are somewhat similar, though the time interval between two episodes of mass loss may be different. Sporadic mass loss and dust condensation with a time scale of a few decades could be a general phenomenon in early M supergiants.

5. Conclusions

We have investigated the circumstellar environment around the supergiant TV Gem from millarcsecond resolution observations in the near infrared using lunar occultation technique. The stellar angular diameter has been determined to be 4.9±0.3 mas and the effective temperature derived is 3670±125 K. Detailed analysis of the occultation light curve has revealed the presence of a circumstellar dust shell at $\sim 20\,R_\star$. In addition, another cooler shell at $\sim 500\,R_\star$ is needed to explain the IRAS photmetric data, particularly at 60 μm. The presence of dust in two isolated shells suggests an episodic or sporadic mass loss in TV Gem. HAR mid infrared observations of this supergiant could throw more light on earlier episodes of mass loss and dust condensation.

Acknowledgements. The authors would like to thank the referee Dr. Andrea Richichi for his useful suggestions which has greatly improved the quality of this paper. The authors are grateful to the Director, Indian Institute of Astrophysics for providing telescope time at Kavalur observatory. We also thank Dr. D.B. Vaidya for making available to us the pre-print of a paper on optical properties of silicate grains. This work was supported by the Department of Space, Government of India.

References

Arnaud K.A., Gilmore G., Cameron A.C., 1989, MNRAS 237, 495
Ashok N.M., Chandrasekhar T., Ragland S., Bhatt H.C., 1994, Experim. Astron. 4, 177
Bester M., Danchi W.C., Degiacomi C.G., Townes C.H., Geballe T.R., 1991, ApJ 367, L27
Bloemhof E.E., Townes C.H., Vanderwyck A.H.B., 1984, ApJ 276, L21
Bloemhof E.E., Danchi W.C., Townes C.H., 1985, ApJ 299, L37
Buss R.H. JR, Snow T.P. Jr, 1988, ApJ 335, 331
Christou J.C., Hebden J.C., Hege E.K., 1988, ApJ 327, 894
Danchi W.C., Bester M., Degiacomi C.G., Greenhill L., Townes C.H., 1994, AJ 107, 1469
Deutsch A.J., 1960, in: Stars and stellar systems, Greenstein J.L. (ed.), Vol 6, chap 15
Draine B.T., Lee H.M., 1984, ApJ 285, 89
Greenberg J.M., Li A., 1996, A&A 309, 258
Gehrz R.D., Woolf N.J., 1971, ApJ 165, 285
Gezari D.Y., Schmitz M., Pitts P.S., Mead J.M., 1993, Catalog of Infrared Observations, NASA, Reference publication 1294

Gillett F.C., Merrill K.M., Stein W.A., 1971, ApJ 165, 285
Hagen W., 1982, PASP 94, 835
Griffin I.P., 1993, MNRAS 260, 831
Heske A., 1990, A&A 229, 494
Hoffleit D., Jaschek C., 1992 in: The bright star catalogue, 4th revised edition. Yale University Observatory
Howell R.R., McCarthy D.W., Low F.J., 1981, ApJ 251, L21
Keenan P.C., Mc Neil R.C., 1989, ApJS 71, 245
Kukarin B.V., et al., 1969, General Catalog of Variable Stars. Moscow: Publ. Office Navka
Loup C., Foryeille T., Omont A., Paul J.F., 1993, A&AS 99, 291
Merrill K.M., Stein W.A., 1976, PASP 88, 285
Nather R.F., McCants N.M., 1970, A.J 75, 963
Onaka T., de Jong T., Willems F.J., 1989, A&A 218, 169
Rowan-Robinson M., Harris S., 1983, MNRAS 202, 767
Radick R.R., Henry G.W., Sherlin J.M., 1984, AJ 89, 151
Richichi A., 1989, A&A 226, 366
Richichi A., 1995 (private communication)
Richichi A., Salinari P., Lisi F., 1988, ApJ 326, 791
Richichi A., Chandrasekhar T., Lisi F., et al., 1995, A&A 301, 439
Ridgway S.T., Wells D.C., Joyce R.R., 1977, AJ 82, 511
Ridgway S.T., Wells D.C., Joyce R.R., Allen R.G., 1979, AJ 84, 247
Roddier C., Roddier F., 1983, ApJ 270, L23
Salpeter E.E., 1974, ApJ 193, 585
Schmidtke P.C., Africano J.L., Jacoby G.H., Joyce R.R., Ridgway S.T., 1986, AJ 91, 961
Schwarzschild M., Härm M., 1962, ApJ 136, 156
Skinner C.J., Whitmore B., 1987, MNRAS 224, 335
Skinner C.J., Whitmore B., 1988, MNRAS 231, 169
Stencel R.E., Pesce J.E., Bauer W.H., 1989, AJ 97, 1120
Sutton E.C., Storey J.W.V., Betz A.L., Townes C.H., Spears D.L., 1977, ApJ 217, L97
Townes C.H., Bester M., Danchi W.C., Degiacomi C.G., Greenhill L.J., 1994, Very High Resolution Imaging. In: Robertson J.G., Tango W.J. (eds.), IAU sym. 158, p. 19
Turner B.E., 1991, ApJ 376, 573
Underhill A.B., 1984, PASP 96, 305
Volk K., Kwok S., 1988, ApJ 331, 435
Winters J.M., Fleischer A.J., Gauger A., Sedlmayr E., 1995, A&A 302, 483
Young K., Phillips T.G., Knapp G.R., 1993, ApJS 86, 517